

# Interactions of lanthanide atoms: Comparative *ab initio* study of YbHe, Yb<sub>2</sub> and TmHe, TmYb potentials

A.A. Buchachenko<sup>1,a</sup>, G. Chałasiński<sup>2,3</sup>, and M.M. Szczyński<sup>3</sup>

<sup>1</sup> Department of Chemistry, Moscow State University, Moscow 119992, Russia

<sup>2</sup> Faculty of Chemistry, Warsaw University, Pasteura 1, 03-093 Warszawa, Poland

<sup>3</sup> Department of Chemistry, Oakland University, Rochester, MI 48309, USA

Received 13 September 2006 / Received in final form 17 October 2006

Published online 8 December 2006 – © EDP Sciences, Società Italiana di Fisica, Springer-Verlag 2007

**Abstract.** The results of high-level *ab initio* calculations are reported for the interatomic potentials describing YbHe, Yb<sub>2</sub>, TmHe and TmYb van der Waals interactions. It is found that the interaction properties of Tm and Yb are very similar and the interaction anisotropy in the TmHe and TmYb complexes is very small. We analyze the long-range behavior of the isotropic and anisotropic interaction potentials and discuss some implications for cold and ultracold atomic collisions of the lanthanide atoms.

**PACS.** 31.25.Nj Electron correlation calculations for diatomic molecules – 34.20.Gj Intermolecular and atom-molecule potentials and forces

## 1 Introduction

It was recently found that the lanthanide atoms (hereafter LN) are very interesting systems for studies of cold and ultracold atomic physics. To mention just a few examples, the first spinless Bose-Einstein condensate was made with Yb atoms [1,2], which opened new possibilities for refined frequency standards [3], accurate measurements of the parity breaking phenomena [4,5], sympathetic cooling of bosonic and fermionic particles [6]. Rare-earth atoms including LN were magnetically trapped in a buffer gas loading experiment [7–9] as a demonstration of the possibility of magnetic trapping of atoms with non-zero electronic orbital angular momenta, and a novel mechanism of laser cooling without repumping has been demonstrated for Er atoms [10].

Theoretical studies of dynamics underpinning these and related phenomena rely on interaction potentials between atoms involved. However, the interactions of LN atoms with each other and foreign gas atoms remain poorly known.

For LN dimers, the current state-of-the-art in experiment and theory is described in a recent review by Lombardi and Davis [11] (see also an earlier review by Morse [12]). The experimental data probe mostly the ground-state potentials near the equilibrium distance and are available only for homonuclear dimers. The most detailed *ab initio* studies to date [13–15] provided valuable insight into the methodology of electronic structure calculations and interactions in a number of homonuclear dimers. They showed, in particular, that, unlike some

other LN dimers, Yb<sub>2</sub> is weakly bound, largely by van der Waals forces. These calculations, however, focused mostly on the equilibrium properties and do not provide any information on long-range interactions particularly important for cold and ultracold collisions.

Even less is known about the van der Waals interactions of LN atoms with foreign gas atoms (among which He is obviously of central importance for cold atom physics). Recently, we have performed an *ab initio* study of the YbHe and TmHe van der Waals complexes [16]. It was demonstrated that the open-shell Tm(<sup>2</sup>F)–He interaction is characterized by very small anisotropy, i.e., very small splitting between the adiabatic states with different electronic orbital angular momentum projection  $\Lambda$ . The suppression of anisotropy of the open inner  $4f$  electronic shell by the closed outer shells, similar to that found in lighter transition metal atoms [8,17], was found to explain observed magnetic trapping of the Tm and other open-shell lanthanides in the buffer-gas loading experiments [9]. The *ab initio* Tm–He interaction potentials have been proven to be accurate enough for an adequate description of the collision dynamics in a magnetic trap at temperatures near 1 K [18]. Another conclusion of reference [16] is a similarity of the isotropic YbHe and TmHe interactions, which, as supported by an empirical analysis of the trapping experiments [19], may be extended to other LNHe systems. These findings have just been confirmed by the time-dependent density functional theory (TDDFT) calculations of the long-range interaction coefficients [20].

The goal of the present paper is to extend previous computational analysis [13,16,21] to obtain a better

<sup>a</sup> e-mail: alexei@classic.chem.msu.su

understanding of van der Waals interactions involving lanthanide atoms. The main questions we are asking are

- (i) Does the similarity in the LN–He interactions extend to LN dimers?
- (ii) How do the interaction strength and the anisotropy depend on the nature of the interaction partner?
- (iii) How do the lanthanide atoms interact at long distances?

We will analyze and compare the open-shell TmHe and TmYb and the closed-shell YbHe and Yb<sub>2</sub> systems. Here Tm(<sup>2</sup>F) represents an open-shell LN atom, while Yb(<sup>1</sup>S) is representative of both a lanthanide and a closed-shell interaction partner. Hence, the comparison of TmYb and Yb<sub>2</sub> is relevant to questions (i) and (iii), while the comparison of TmHe, YbHe and TmYb, Yb<sub>2</sub> pairs provides an indication for (ii). In addition, a comparison with the previous data may allow for an instructive assessment of the ab initio methods used.

## 2 Calculation details

The ab initio methods applied here were the same as we used in reference [16].

For both the Yb and Tm atoms we used the small-core relativistic effective core potentials ECP28MWB [22]. They describe 28 electrons belonging to the inner shells with the principal quantum numbers  $n = 1-3$ . The rest of the electrons were treated explicitly using the supplementary atomic natural orbital (ANO) ( $14s13p10d8f6g/6s6p5d4f3g$ ) basis sets [23]. These bases are known to poorly describe the polarization properties of LN atoms and must for the present purposes be augmented by diffuse functions [13,16,21]. Major improvement can be achieved by adding just a single diffuse  $p$  function to polarize the external  $6s$  shell which gives the dominant contribution to the LN polarizability, while the diffuse functions with higher orbital angular momenta further improve the convergence [16,21]. Here we used two atom-centered augmentations. The first one included  $p$  and  $d$  functions with the exponents 0.028 and 0.032, as optimized for the polarizability of Yb [16]. The second  $2pdfg$  set (the exponents are 0.028 and 0.015 for  $p$ , 0.032 for  $d$  and 0.05 for  $f$  and  $g$  functions) has been suggested recently for better convergence of the polarizability of Yb and the dispersion interaction of Yb with He [21]. In what follows the resulting basis sets will be denoted as ANO+ $pd$  and ANO+ $2pdfg$ , respectively. For the LNHe calculations, we used the ANO+ $pd$  basis in combination with the augmented correlation-consistent quadruple-zeta aug-cc-pVQZ basis for He, while the ANO+ $2pdfg$  basis was combined with a larger quintuple-zeta aug-cc-pV5Z set [24]. In a few cases (marked as “+ $bf$ ”), the set of the bond functions was placed at the midpoint of the internuclear distance  $R$ . The  $bf$  set consisted of  $3s3p2d2f1g$  functions with the exponents from reference [25].

Two types of correlated calculations, in the single-reference (SR) and multi-reference (MR) frames, were performed depending on the nature of the interaction. The

MR approach to the open-shell systems involving the Tm atom consisted of complete active space multiconfiguration self-consistent field (CASSCF) calculations followed by averaged quadratic coupled cluster (AQCC) calculations, as used for TmHe in reference [16]. For TmYb, the complete active space for 31 electrons involved 16 molecular orbitals (MO’s) correlating to the  $4f$  and  $6s$  atomic orbitals (AO’s) of both partners. MO’s with lower orbital energies correlating to  $4s$ ,  $4p$ ,  $4d$ ,  $5s$  and  $5p$  AO’s were kept doubly occupied. State averaging was performed over all seven components of the  $^2\Sigma^+$ ,  $^2\Pi$ ,  $^2\Delta$ ,  $^2\Phi$  adiabatic states arising from the  $^2F$  atomic state in the axial symmetry. Special care was taken to generate CASSCF wave functions corresponding to the proper expectation values of the projection  $A$  of the electronic orbital angular momentum  $L$  onto the internuclear axis. In the subsequent AQCC calculations, the lowest 18 MO’s (correlating to  $4s$ ,  $4p$  and  $4d$  AO’s) were kept in the core, 2 MO’s (correlating to  $5s$  AO’s) were kept correlated but doubly occupied, while 22 MO’s (correlating to  $5p$ ,  $4f$  and  $6s$  AO’s) were treated as active. Each adiabatic state was calculated separately on a grid of the internuclear distances  $R$  up to 25 Å. The interaction potentials  $V_A(R)$  were obtained using the supermolecular formula [26] accounting for the counterpoise correction for each state individually. For TmHe, correlation was treated in the same manner, but only one MO of interaction partner related to  $1s$  AO of He entered the active subspace [16].

To keep close correspondence with the above MR calculations for Tm-containing systems, YbHe and Yb<sub>2</sub> were also studied within the AQCC method using the same partitioning of the MO space, with the only difference that the restricted SCF MO’s now represented the reference. The SR calculations were also performed using the restricted coupled cluster method with single and double excitations and non-iterative correction to triple excitations, RCCSD(T). This approach allowed us to augment a basis set by bond functions. In addition, we report some preliminary results obtained for Yb<sub>2</sub> with the symmetry-adapted perturbation theory based on the density functional treatment of monomers, SAPT(DFT) [27,28]. The PBE0 DFT functional asymptotically corrected according to reference [29] and ANO+ $2pdfg$  basis set were used for Yb atom.

All ab initio calculations were made with MOLPRO program package [30].

## 3 Ab initio interaction potentials

### 3.1 Adiabatic and anisotropic interactions

Interactions involving open-shell atom(s) with non-zero orbital angular momentum  $L$  can be described using two convenient representations. Scalar-relativistic ab initio calculations based on the standard Born-Oppenheimer approximation result in the adiabatic potentials  $V_A(R)$  labelled by the quantum number  $A = \Sigma, \Pi, \Delta, \dots$  — the projection of  $L$  on the internuclear axis. Alternatively, the interaction potential operator can be expanded in Legendre

**Table 1.** Equilibrium and long-range parameters of the TmHe and YbHe interactions for the adiabatic electronic states and the lowest  $\lambda = 0, 2$  terms of the anisotropic expansion. The number of decimal digits is chosen to stress the difference in the parameters of quasi-degenerated adiabatic states.

Method/basis	State	$R_e, \text{\AA}$	$D_e, \text{cm}^{-1}$	$C_6^A, \text{a.u.}$	$C_{6,0}, \text{a.u.}$	$C_{6,2}, \text{a.u.}$
TmHe						
AQCC/ANO+ $pd^a$	$^2\Sigma^+$	6.175	2.358	41.17	-	-
	$^2\Pi$	6.177	2.353	41.17	-	-
	$^2\Delta$	6.178	2.353	41.21	-	-
	$^2\Phi$	6.172	2.363	41.11	-	-
	$\lambda = 0$	6.176	2.356	-	41.17	-
	$\lambda = 2$	-	-	-	-	0.10
	AQCC/ANO+ $2pdfg$	$^2\Sigma^+$	6.118	2.948	41.82	-
$^2\Pi$		6.079	3.055	41.78	-	-
$^2\Delta$		6.066	3.066	41.79	-	-
$^2\Phi$		6.068	3.071	41.72	-	-
$\lambda = 0$		6.082	3.047	-	41.77	-
$\lambda = 2$		-	-	-	-	0.14
TDDFT <sup>b</sup>		$\lambda = 0, 2$	-	-	-	37.92
YbHe						
AQCC/ANO+ $pd$	$^1\Sigma^+$	6.183	2.345	40.1	40.1	0.0
RCCSD(T)/ANO+ $pd^a$	$^1\Sigma^+$	6.135	2.463	44.3	44.3	0.0
AQCC/ANO+ $2pdfg$	$^1\Sigma^+$	6.076	3.051	42.3	42.3	0.0
RCCSD/ANO+ $2pdfg$	$^1\Sigma^+$	6.159	2.331	38.5	38.5	0.0
RCCSD(T)/ANO+ $2pdfg$	$^1\Sigma^+$	5.934	3.250	44.5	44.5	0.0
RCCSD(T)/ANO+ $2pdfg+bf$	$^1\Sigma^+$	5.886	3.578	-	-	0.0
TDDFT <sup>b</sup>	$^1\Sigma^+$	-	-	-	37.28	0.0

<sup>a</sup> Reference [16]; <sup>b</sup> reference [20].

polynomials as the functions of the angle that specifies the orientation of the non-spherical electronic cloud with respect to the same axis [31]. These two representations are equivalent and uniquely interrelated [31,32]. For the Tm atom in the ground  $^2F$  state interacting with a spherical particle (e.g., He or Yb atom in the  $^1S$  state) the set of four adiabatic potentials for  $^2\Sigma^+$ ,  $^2\Pi$ ,  $^2\Delta$  and  $^2\Phi$  states determines four coefficients in the anisotropic Legendre expansion  $V_\lambda(R)$  with  $\lambda = 0, 2, 4, 6$  [16]. The explicit expressions for the isotropic and the lowest anisotropic terms  $\lambda = 0$  and  $\lambda = 2$  are

$$\begin{aligned} V_0 &= (V_\Sigma + 2V_\Pi + 2V_\Delta + 2V_\Phi)/7 \\ V_2 &= 5(V_\Sigma - V_\Phi)/7 + 15(V_\Pi - V_\Delta)/14. \end{aligned} \quad (1)$$

Note that only these two terms contain the contributions to the  $C_{6,0}$  and  $C_{6,2}$  dispersion coefficients of the  $-1/R^6$  term dominating the long-range interactions in the cases considered here.

The interaction of two closed-shell atoms gives rise to a single adiabatic state with  $\Lambda = \Sigma$  and it is therefore isotropic ( $V_0 = V_\Sigma$ ). For instance, the YbHe and Yb<sub>2</sub> systems have the ground state of  $^1\Sigma^+$  symmetry.

### 3.2 TmHe and YbHe interactions

The interactions of Tm and Yb atoms with He were analyzed in detail in reference [16] and the present calculations provide quantitative improvement owing to better saturated basis sets.

The parameters of the ab initio adiabatic potentials  $V_\Lambda$  are listed in Table 1. The equilibrium distances  $R_e$  and the well depths  $D_e$  were obtained through the cubic spline interpolation of the ab initio points, whereas the lowest-order dispersion coefficients  $C_6^A$  were fit to a long-range part of the calculated interaction energy (typically  $R \geq 15 \text{\AA}$ ) using the  $-C_6^A/R^6$  dependence. In the case of TmHe, the same parameters are presented for the isotropic  $\lambda = 0$  term  $V_0$ , while for the lowest anisotropic  $\lambda = 2$  term  $V_2$  only the  $C_{6,2}$  coefficient is given (see reference [16] for more details on the behavior of  $V_2$  as well as the higher anisotropic terms).

Comparing to the previous calculations with the ANO+ $pd$  basis set, the use of the ANO+ $2pdfg$  basis gives remarkably shorter (by ca. 0.1  $\text{\AA}$ ) equilibrium distances and deeper (by ca. 30%) potential wells. The variation of the dispersion coefficients is not so large. These changes are practically the same for both TmHe and YbHe systems and their isotropic potentials (compared at the AQCC level of theory) stay very close to each other near the van der Waals minimum and at long distances.

Some additional comments are in order. First, the present results confirm that the correlation treatment including single and double excitations is not enough to reproduce well the weak bonding by dispersion forces [33]. Though for the YbHe interaction the AQCC treatment is superior over the RCCSD one, the non-iterative triple correction implemented within the RCCSD(T) method remarkably improves the values of equilibrium parameters and dispersion coefficients. Second, there are some

**Table 2.** Equilibrium and long-range parameters of the TmYb and Yb<sub>2</sub> interactions for the adiabatic electronic states and the lowest  $\lambda = 0, 2$  terms of the anisotropic expansion. The number of decimal digits is chosen to stress the difference in the parameters of quasi-degenerated adiabatic states.

Method/basis	State	$R_e, \text{\AA}$	$D_e, \text{cm}^{-1}$	$C_6^A, \text{a.u.}$	$C_{6,0}, \text{a.u.}$	$C_{6,2}, \text{a.u.}$
TmYb						
AQCC/ANO+ <i>pd</i>	$^2\Sigma^+$	5.136	216.0	1800.6	-	-
	$^2\Pi$	5.137	216.5	1800.6	-	-
	$^2\Delta$	5.112	227.0	1803.4	-	-
	$^2\Phi$	5.148	211.2	1795.7	-	-
	$\lambda = 0$	5.132	217.8	-	1800.0	-
	$\lambda = 2$	-	-	-	-	8.7
AQCC/ANO+2 <i>pdfg</i>	$^2\Sigma^+$	5.079	323.8	2174.6	-	-
	$^2\Pi$	5.071	327.6	2174.6	-	-
	$^2\Delta$	5.034	337.2	2176.4	-	-
	$^2\Phi$	5.095	314.5	2166.3	-	-
	$\lambda = 0$	5.070	326.0	-	2172.6	-
	$\lambda = 2$	-	-	-	-	14.6
Yb <sub>2</sub>						
AQCC/ANO+ <i>pd</i>	$^1\Sigma^+$	5.127	216.6	1801.1	1801.1	0.0
RCCSD(T)/ANO+ <i>pd</i> <sup>a</sup>	$^1\Sigma^+$	4.857	377.4	2163.4	2163.4	0.0
AQCC/ANO+2 <i>pdfg</i>	$^1\Sigma^+$	5.056	321.7	2158.0	2158.0	0.0
SAPT(DFT)/ANO+2 <i>pdfg</i>	$^1\Sigma^+$	-	-	2416.7	2416.7	0.0
RCCSD/ANO+2 <i>pdfg</i>	$^1\Sigma^+$	5.066	311.8	1873.6	1873.6	0.0
RCCSD(T)/ANO+2 <i>pdfg</i>	$^1\Sigma^+$	4.809	538.3	2567.9	2567.9	0.0
RCCSD(T)/ANO+2 <i>pdfg</i> + <i>bf</i>	$^1\Sigma^+$	4.472	723.7	-	-	0.0
RCCSD(T)/ANO+3 <i>s3p3d3f3g</i> <sup>b</sup>	$^1\Sigma^+$	4.549	742.0	-	-	0.0
RCCSD(T), large core <sup>c</sup>	$^1\Sigma^+$	4.861	467.8	-	-	0.0

<sup>a</sup> Reference [16]; <sup>b</sup> reference [14]; <sup>c</sup> reference [13], calculations with the large-core ECP.

indications that the basis set may still not be fully saturated. Bond functions are known to be very efficient to account for the dispersion interaction near the van der Waals minimum [34,35]. The result of the RCCSD(T)/ANO+2*pdfg*+*bf* calculations for YbHe demonstrates that the inclusion of the bond functions indeed affects the equilibrium parameters to a great extent. However, the *bf* augmentation is not adequate at long distances and is not advised for the MR correlated calculations [36]. Finally, it is interesting to compare the present ab initio and long-range time-dependent density functional calculations [20]. The  $C_{6,0}$  coefficients from reference [20] for both TmHe and YbHe interactions are slightly smaller than ours, but still very similar, while the  $C_{6,2}$  coefficient for TmHe is three times larger. A similar disagreement was noted before for the ScHe interaction [37].

### 3.3 TmYb and Yb<sub>2</sub> interactions

The parameters of the calculated TmYb and Yb<sub>2</sub> interaction potentials obtained in the same way as for the TmHe and YbHe systems are presented in Table 2.

The accuracy of various ab initio approaches can be easily assessed for ytterbium dimer. A better saturation of the basis set by the diffuse component from +*pd* to +2*pdfg* provides a significant effect: the  $R_e$  value is reduced by 0.07 (0.05)  $\text{\AA}$ , the  $D_e$  and  $C_6$  values increase by 49 (43) and 20 (19)%, respectively, at the AQCC

(RCCSD(T)) level of theory. However, the effect of the extensive correlation treatment is even more pronounced: the  $R_e$  value is reduced by 0.25  $\text{\AA}$ ,  $D_e$  and  $C_6$  values increase by 67 and 19%, respectively, when passing from the AQCC to the RCCSD(T) correlated calculations with the same ANO+2*pdfg* basis set. The ANO+2*pdfg* basis is itself not fully saturated: the RCCSD(T) calculations with the same ANO basis massively augmented by the 3*s3p3d3f3g* diffuse set [14] further reduce the equilibrium distance and increase the interaction strength. Present calculations with the bond functions provide the same evidence. We should conclude that the present results cannot be regarded as fully converged and that the convergency reached for TmYb and Yb<sub>2</sub> systems is worse than that for TmHe and YbHe. Ytterbium dimer was also carefully studied by Wang and Dolg [13] using various ab initio schemes. These authors concluded that the RCCSD(T) calculations with a large-core relativistic effective core pseudopotential for 60 inner electrons and core-polarization potentials give the best results (shown in Tab. 2 as “large core”) that fall in between our AQCC and RCCSD(T)/ANO+2*pdfg* data.

The AQCC results for the anisotropic TmYb interaction vary similarly with the extension of the basis set as for TmHe and Yb<sub>2</sub>: the equilibrium distance becomes shorter, the well depth and dispersion interaction become larger, the interaction anisotropy becomes more pronounced. Indeed, the absolute magnitude of interaction anisotropy is much larger for TmYb than TmHe. Near

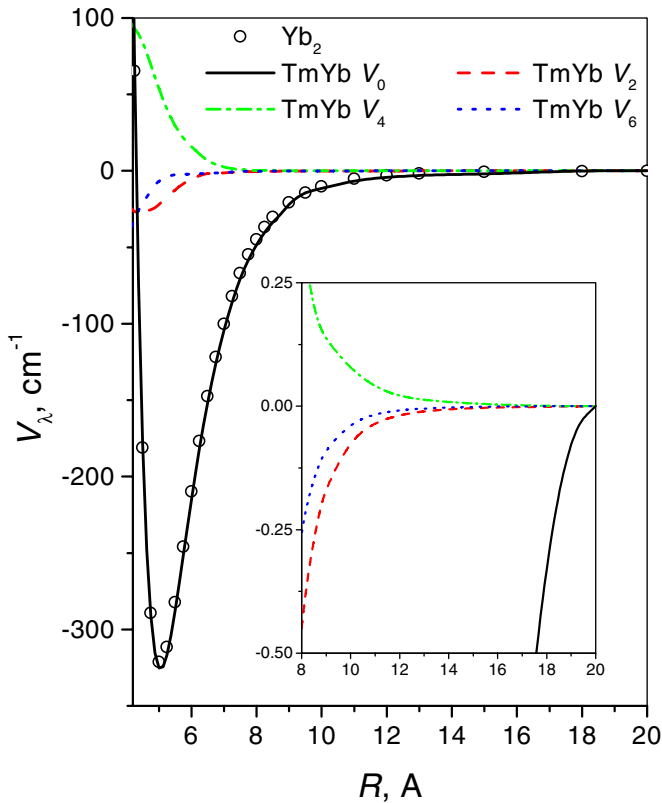


**Fig. 1.** (Color online) Radial dependences of the  $V_\lambda$  terms of the TmYb interactions. Isotropic  $\text{Yb}_2$  potential is also shown for comparison. Inset emphasizes the long-range behavior.

the equilibrium, the manifold of TmYb adiabatic states spans ca.  $22.7 \text{ cm}^{-1}$ , while the TmHe states are degenerate to within ca.  $0.12 \text{ cm}^{-1}$  (AQCC+2pdfg data). The relative anisotropy (measured as the ratio of the splitting to the well depth of the isotropic potential) is also higher for TmYb — 7% vs. 4%. Figure 1, in which the radial dependences of the Legendre coefficients  $V_\lambda$  ( $\lambda = 0, 2, 4, 6$ ) are plotted, indicates that one reason may be the contribution of higher anisotropic terms through high-order dispersion interaction components.

The most important result of Figure 1 and Table 2 is the close similarity between  $\text{Yb}_2$  and the isotropic TmYb potentials computed at the same level of theory. The relative difference in  $R_e$ ,  $D_e$  and  $C_{6,0}$  does not exceed 0.3, 1.3 and 0.7%, respectively, being practically the same as in the TmHe and YbHe interactions.

### 3.4 Long-range interactions

The most important implication of the present calculations to the field of cold and ultracold atomic collision is the estimation of the long-range interactions. Static dipole polarizabilities for LN atoms, isotropic (scalar)  $\alpha_0^{\text{LN}}$  and anisotropic (tensor)  $\alpha_2^{\text{LN}}$ , were calculated using the same ab initio approaches in reference [21] and are presented in Table 3, whereas for He we accepted the experimental value  $\alpha^{\text{He}} = 1.38 \text{ a.u.}$  (see, e.g., Ref. [38]), which is well

reproduced within the present ab initio description of the He atom.

The  $C_6$  coefficient of the leading  $-1/R^6$  long-range potential energy term for two neutral atoms corresponds to the interaction between two induced dipoles and is given by the convolution of the atomic dynamic polarizabilities  $\alpha(i\omega)$  over the (imaginary) frequency (see, e.g., Ref. [39]). Static polarizability approximation relates the  $C_6$  coefficients to the product of static dipole polarizabilities at  $\omega = 0$ . It follows from Tables 1 and 2 that the isotropic  $C_{6,0}$  coefficient increases from LNHe to LNYb by 50 times, whereas the ratio of the static polarizabilities for He and Yb is about 110. More accurate dependence of the  $C_{6,0}$  coefficient on the static polarizabilities of the partners is given by the well-known Slater-Kirkwood (SK) formula [40]:

$$C_{6,0}(\text{LN} - \text{A}) = \frac{3}{2} \frac{U_{\text{LN}} U_{\text{A}}}{U_{\text{LN}} + U_{\text{A}}} \alpha_0^{\text{LN}} \alpha^{\text{A}}, \quad (2)$$

where  $U_{\text{LN}}$  and  $U_{\text{A}}$  are the effective excitation energies of LN and A atoms

$$U_{\text{A}} = (N_{\text{A}}/\alpha^{\text{A}})^{1/2}, \quad U_{\text{LN}} = (N_{\text{LN}}/\alpha_0^{\text{LN}})^{1/2}. \quad (3)$$

Here  $N$  is interpreted as an effective number of electrons. For the He atom, the empirical value  $N_{\text{He}} = 1.434$  can be found in the literature (e.g., in Ref. [38]). The Slater-Kirkwood parameters for LN atoms are not known, but can be estimated from the present calculations inverting equation (2) (for TmHe and YbHe) and/or using the simplified SK formula for a homonuclear molecule (for  $\text{Yb}_2$ ):

$$C_{6,0}(\text{LN}_2) = \frac{3}{4} U_{\text{LN}} (\alpha_0^{\text{LN}})^2. \quad (4)$$

The resulting SK parameters are listed in Table 3. The value of  $N_{\text{Yb}}$  obtained from  $\text{Yb}_2$  interaction depends much stronger on the ab initio approach than that derived from the data for YbHe, as a result of better convergence achieved in the latter case. The values of  $N_{\text{LN}}$  for Tm and Yb are similar. We conclude that the effective number of electrons contributing to the dipole polarizability of these atoms is 3.5–4, which means that not more than two electrons from the inner shells may respond to an external electric field. (The TDDFT calculations [20] give even smaller values: for all LN atoms  $N_{\text{LN}}$  varies from 2.6 to 3.2.)

Using the best value of  $N_{\text{Yb}}$  from the YbHe RCCSD(T)/ANO+2pdfg calculations, the converged value of the  $\text{Yb}_2$   $C_{6,0}$  coefficient can be estimated to be 2850 a.u., 10% above that computed at the same level of theory (2570 a.u., Tab. 2) and using the SAPT(DFT) (2420 a.u.). These values markedly exceed the range of 1000–2000 a.u. accepted in reference [1] as derived from the first allowed dipole transition.

The known anisotropic long-range coefficients  $C_{6,2}$  for the lanthanides (as well as for other transition metal atoms like Ti and Sc [7, 8, 17, 37]) are very small [16, 19, 20]. Within the orbital picture this is interpreted by screening of the unpaired electrons occupying the inner  $f$  or  $d$  shells

**Table 3.** Ab initio polarizability values [21] and Slater-Kirkwood parameters  $U_{LN}$  and  $N_{LN}$  derived from the present YbHe, Yb<sub>2</sub> and TmHe calculations.

Atom	System	Method/basis	$\alpha_0^{LN}$ ( $\alpha_2^{LN}$ ), a.u.	$U_{LN}$	$N_{LN}$
Yb	Yb <sub>2</sub>	AQCC/ANO+ <i>pd</i>	151.9	0.10	1.65
		AQCC/ANO+2 <i>pdfg</i>	152.7	0.12	2.33
		RCCSD(T)/ANO+2 <i>pdfg</i>	153.2	0.15	3.26
Yb	YbHe	AQCC/ANO+ <i>pd</i>	151.9	0.15	3.21
		AQCC/ANO+2 <i>pdfg</i>	152.7	0.15	3.61
		RCCSD(T)/ANO+2 <i>pdfg</i>	153.2	0.16	4.04
Tm	TmHe	AQCC/ANO+ <i>pd</i>	152.4 (−2.1)	0.15	3.21
		AQCC/ANO+2 <i>pdfg</i>	153.3 (−2.3)	0.15	3.61

by the closed spherical outer *s* shell. The present calculations show that this trend holds not only for interactions with He, but also for the TmYb lanthanide dimer.

The relative anisotropy can be characterized by the ratio of the anisotropic to isotropic dispersion interaction strengths  $\chi = C_{6,2}/C_{6,0}$ . Within the static polarizability approximation  $\chi \approx -(3/2)\alpha_2^{Tm}/\alpha_0^{Tm}$  [20,19,16]. The anisotropy of the dipole polarizability is also suppressed (which follows not only from the abovementioned theoretical calculations, but also from the direct experimental measurements [41,42]), so the value of  $\chi$  for Tm estimated using the calculated polarizabilities from Table 3 is as small as 0.022. Yet, the real values of  $\chi$  are even smaller: the present AQCC/ANO+2*pdfg* calculations give 0.003 for TmHe and 0.007 for TmYb. The reason for that is a faster decay of the tensor polarizability component with imaginary frequency, which further decreases  $C_{6,2}$  with respect to  $C_{6,0}$  [20,37]. At the same time, the present calculations indicate that the ratio of the anisotropic  $C_{6,2}$  coefficients for TmYb and TmHe systems (104) matches the ratio of the Yb and He polarizabilities (110) much better than does the ratio of the  $C_{6,0}$  coefficients. This is again in agreement with the results of references [20,37]: fast decay of the dynamic  $\alpha_2^{LN}$  polarizability with  $\omega$  makes it look like a Dirac  $\delta$ -function for which the static polarizability approximation is valid.

## 4 Concluding remarks

We have reported high-level ab initio calculations of the interaction potentials for the van der Waals complexes TmYb, Yb<sub>2</sub>, TmHe and YbHe. The results for TmYb are, to the best of our knowledge, the first for a heteronuclear lanthanide dimer, while the calculations for TmHe and YbHe improve upon the previous data. We emphasize several findings that may be important for understanding general trends in the interactions involving LN atoms, implications for cold and ultracold atomic physics and applicability of the ab initio quantum chemistry methods.

(i) The interactions of Yb and Tm atoms with He are very weak and very similar. Based on the previous works [9,16,19,20], it is reasonable to suggest that the isotropic interactions for all the LNHe family are similar and close to that computed here for YbHe at the RCCSD(T)/ANO+2*pdfg* level of theory.

- (ii) The suppression of the interaction anisotropy makes the TmHe potential very isotropic. Improvement of the ab initio calculations revealed larger anisotropy than was obtained before [16,19], in agreement with the results of the scattering calculations on the Zeeman relaxation rates, which indicate an underestimation of the anisotropy in the previous AQCC/ANO+*pd* ab initio potentials [18].
- (iii) The isotropic interactions of the TmYb and Yb<sub>2</sub> dimers are also very similar. This indicates the possibility of sympathetic cooling of open-shell LN atoms in an ultracold gas of ytterbium, if such similarity extends to other LNYb systems.
- (iv) The suppression of the interaction anisotropy manifests itself also in the TmYb system. Though we found that the absolute anisotropy increases from TmHe to TmYb by more than two orders of magnitude depending on the internuclear distance, the relative anisotropy, which is often more important [9,18], increases only by a factor of three. The growth of the relative long-range anisotropy with the polarizability of the interaction partner originates from the different behavior of the isotropic  $C_{6,0}$  and anisotropic  $C_{6,2}$  coefficients. The latter varies linearly, in accord with the static polarizability approximation, while increase of the  $C_{6,0}$  value with the static anisotropy of the partner is markedly slower.
- (v) Analysis of the long-range interactions involving LN atoms using the Slater-Kirkwood formula indicates a very small contribution of the inner electronic shells into the dispersion interaction. We conclude that the value of the  $C_6$  dispersion coefficient for Yb<sub>2</sub> falls within a range 2400–2800 a.u., being significantly larger than was suggested previously (1000–2000 a.u.) [1].
- (vi) Incomplete convergency, most clearly seen for Yb<sub>2</sub> results, indicates the need for more advanced ab initio schemes, first of all, better accounting for correlation effects in multi-reference wave functions (e.g., within MR coupled cluster method). For highly accurate calculations further improvements of the basis set may also be helpful.

We thank Roman Krems for instructive comments and Xi Chu and Gerrit C. Groenenboom for sharing with us their TDDFT results. The work was supported by the U.S. National

Science Foundation (Grant No. CHE-0414241), the University of British Columbia (AAB) and the Russian Science Support Foundation (AAB).

## References

1. Y. Takasu, K. Honda, K. Komori, T. Kuwamoto, M. Kumakura, Y. Takahashi, T. Yabuzaki, *Phys. Rev. Lett.* **90**, 023003 (2003)
2. Y. Takasu, K. Maki, K. Komori, T. Takano, K. Honda, M. Kumakura, T. Yabuzaki, Y. Takahashi, *Phys. Rev. Lett.* **91**, 040404 (2003)
3. J.L. Hall, M. Zhu, P. Buch, *J. Opt. Soc. Am. B* **6**, 2194 (1989)
4. D. DeMille, *Phys. Rev. Lett.* **74**, 4165 (1995)
5. J.E. Stalnaker, D. Budker, S.J. Freedman, J.S. Guzman, S.M. Rochester, V.V. Yashchuk, *Phys. Rev. A* **73**, 043416 (2006)
6. K. Honda, Y. Takasu, T. Kuwamoto, M. Kumakura, Y. Takahashi, T. Yabuzaki, *Phys. Rev. A* **66**, 021401 (R) (2002)
7. C.I. Hancox, S.C. Doret, M.T. Hummon, R.V. Krems, J.M. Doyle, *Phys. Rev. Lett.* **94**, 013201 (2005)
8. R.V. Krems, J. Kłos, M.F. Rode, M.M. Szczyński, G. Chałasiński, A. Dalgarno, *Phys. Rev. Lett.* **94**, 013202 (2005)
9. C.I. Hancox, S.C. Doret, M.T. Hummon, L. Luo, J.M. Doyle, *Nature* **431**, 281 (2004)
10. J.J. McClelland, J.L. Hanssen, *Phys. Rev. Lett.* **96**, 143005 (2006)
11. J.R. Lombardi, B. Davis, *Chem. Rev.* **102**, 2431 (2002)
12. M.D. Morse, *Chem. Rev.* **86**, 1049 (1986)
13. Y. Wang, M. Dolg, *Theor. Chem. Acc.* **100**, 124 (1998)
14. X. Cao, M. Dolg, *Theor. Chem. Acc.* **108**, 143 (2002)
15. X. Cao, M. Dolg, *Mol. Phys.* **101**, 1967 (2003)
16. A.A. Buchachenko, M.M. Szczyński, G. Chałasiński, *J. Chem. Phys.* **124**, 114301 (2006)
17. J. Kłos, M.F. Rode, J.E. Rode, G. Chałasiński, M.M. Szczyński, *Eur. Phys. J. D* **31**, 429 (2004)
18. A.A. Buchachenko, G. Chałasiński, M.M. Szczyński, R.V. Krems, *Phys. Rev. A* **74**, 022705 (2006)
19. R.V. Krems, A.A. Buchachenko, *J. Chem. Phys.* **123**, 101101 (2005)
20. X. Chu, G.C. Groenenboom, A. Dalgarno, in preparation
21. A.A. Buchachenko, J. Kłos, G. Chałasiński, M.M. Szczyński, unpublished
22. M. Dolg, H. Stroll, H. Preuss, *J. Chem. Phys.* **90**, 1730 (1989)
23. X. Cao, M. Dolg, *J. Chem. Phys.* **115**, 7348 (2001)
24. D.E. Woon, T.H. Dunning Jr, *J. Chem. Phys.* **100**, 2975 (1994)
25. S.M. Cybulski, R.R. Toczyłowski, *J. Chem. Phys.* **111**, 10520 (1999)
26. M.H. Alexander, *J. Chem. Phys.* **108**, 4467 (1998)
27. A. Hesselman, G. Jansen, *Chem. Phys. Lett.* **357**, 464 (2002)
28. A. Misquitta, B. Jeziorski, K. Szalewicz, *Phys. Rev. Lett.* **41**, 033201 (2003)
29. M. Grüning, O.V. Gritsenko, S.J.A. Gisbergen, E.J. Baerends, *J. Chem. Phys.* **114**, 652 (2001)
30. H.-J. Werner, P.J. Knolwes, R. Lindh, F.R. Manby, M. Schütz and others, MOLPRO, versions 2002.6 and 2006.1, a package of ab initio programs, see <http://www.molpro.net>, Cardiff, UK, 2006
31. V. Aquilanti, G. Grossi, *J. Chem. Phys.* **73**, 1165 (1980)
32. R.V. Krems, G.C. Groenenboom, A. Dalgarno, *J. Phys. Chem. A* **108**, 8941 (2004)
33. J.A. Kłos, G. Chałasiński, M.M. Szczyński, H.-J. Werner, *J. Chem. Phys.* **115**, 3085 (2001)
34. G. Chałasiński, M.M. Szczyński, *Chem. Rev.* **94**, 1723 (1994)
35. G. Chałasiński, M.M. Szczyński, *Chem. Rev.* **100**, 4227 (2000)
36. J. Kłos, G. Chałasiński, M.M. Szczyński, *Int. Rev. Phys. Chem.* **23**, 541 (2004)
37. X. Chu, G.C. Groenenboom, A. Dalgarno, *Phys. Rev. A* **72**, 032703 (2005)
38. A.D. Koutselos, E.A. Mason, L.A. Viehland, *J. Chem. Phys.* **93**, 7125 (1990)
39. A.J. Stone, *The Theory of Intermolecular Forces* (Clarendon Press, Oxford, 1996)
40. J.C. Slater, J.G. Kirkwood, *Phys. Rev.* **37**, 682 (1931)
41. R.-H. Rinkleff, F. Thorn, *Z. Phys. D* **31**, 31 (1994)
42. R.-H. Rinkleff, F. Thorn, *Z. Phys. D* **32**, 173 (1994)